EFFECT OF ENERGY DEPOSITION MODELLING IN COUPLED STEADY STATE MONTE CARLO NEUTRONICS/THERMAL HYDRAULICS CALCULATIONS

Riku Tuominen[1], Ville Valtavirta[1], Manuel García[2], Diego Ferraro[2] and Jaakko Leppänen[1]
[1]VTT Technical Research Centre of Finland Ltd
P.O Box 1000, FI-02044 VTT, Finland

[2]Karlsruhe Institute of Technology, Institute of Neutron Physics and Reactor Technology
Hermann-von-Helmholtz-Platz 1, 76344 Eggenstein-Leopoldshafen, Germany

riku.tuominen@vtt.fi

ABSTRACT

In coupled calculations with Monte Carlo neutronics and thermal hydraulics the Monte Carlo code is used to produce a power distribution which in practice means tallying the energy deposition. Usually the energy deposition is estimated by making a simple approximation that energy is deposited only in fission reactions. The goal of this work is to study how the accuracy of energy deposition modelling affects the results of steady state coupled calculations. For this task an internal coupling between Monte Carlo transport code Serpent 2 and subchannel code SUBCHANFLOW is used along with a recently implemented energy deposition treatment of Serpent 2. The new treatment offers four energy deposition modes each of which offers a different combination of accuracy and required computational time. As a test case, a 3D PWR fuel assembly is modelled with different energy deposition modes. The resulting effective multiplication factors are within 30 pcm. Differences of up to 100 K are observed in the fuel temperatures.

KEYWORDS: Monte Carlo, multi-physics, energy deposition, Serpent, SUBCHANFLOW

1. INTRODUCTION

In the recent years with the increase in the available computational resources, there has been a strong interest to develop high definition approaches to tackle coupled neutronics/thermal hydraulics problems. The thermal hydraulics part of these problems is usually solved with CFD or subchannel codes and neutronics with Monte Carlo codes. To be more specific in the coupled calculations the Monte Carlo code is used to produce a power distribution which in practise means tallying the energy deposition. This task can be achieved using different methods having varying accuracy. As an example, a simple method, which has been used widely in coupled calculations, assumes that all energy is deposited locally at fission sites even though fission neutrons and gammas transport energy away from the fission site and deposit it elsewhere. In addition, fission reactions are not the only reactions that release additional energy. Especially radiative capture reactions usually contribute a non-negligible amount to the total energy release.

Recently a new energy deposition treatment was implemented to the Monte Carlo transport code Serpent 2. Four energy deposition modes are available and each of the energy deposition modes offers a different combination of accuracy and required computational time. By using these modes and an internal coupling with the subchannel code SUBCHANFLOW the effect of energy deposition modelling on fuel temperatures in steady state coupled calculations is studied. As a test case, a 3D PWR fuel assembly is modelled. The test case is solved with different energy deposition modes and the resulting fuel temperatures are compared along with effective multiplication factors and total calculation times.

2. METHODS

2.1. Serpent

Serpent [1] is a state-of-the-art Monte Carlo transport code developed at VTT Technical Research Centre of Finland Ltd since 2004. The code was originally written for spatial homogenization in reactor applications but has gained many additional features over the years of development. These include a built-in burnup calculation capability, photon transport [2] and a multi-physics interface which allows coupling to external CFD, thermal hydraulics and fuel performance codes [3]. A development version based on Serpent 2.1.31 was used in this work.

2.2. SUBCHANFLOW

SUBCHANFLOW (SCF) is a subchannel thermal-hydraulic code for steady state and transient analysis of nuclear reactors developed at KIT [4]. The code solves liquid-vapor mixture equations for the conservation of mass, momentum and energy. In addition, heat conduction in fuel rods can be solved and the code features simplified models for cracking, swelling, gap conductance etc.

2.3. Coupling

The calculations presented in this paper use an internal coupling between Serpent and SCF. The coupling is based on master-slave approach with Serpent acting as a master and SCF as a slave. Serpent executes the necessary SCF routines when a new thermal-hydraulic solution is needed. The implementation of the internal coupling is described in more detail in [5].

2.4. Energy Deposition Modes

Recently a new energy deposition treatment was implemented to Serpent 2 [6]. The user has the ability to choose an energy deposition mode based on the user's needs and each mode offers a different combination of spatial accuracy and required computational time. In the following, these four energy deposition modes are introduced briefly. A more thorough description can be found in [6].

2.4.1. Mode 0: constant energy deposition per fission

This is the default mode in Serpent and the employed methodology has been used in the previous versions of Serpent to calculate the fission energy deposition. All energy is deposited locally at

fission sites and the energy deposition per fission for nuclide i is calculated as

$$E_{\text{fiss},i} = \frac{Q_i}{Q_{235}} H_{235}, \tag{1}$$

where Q_i is the fission Q-value for nuclide i, Q_{235} the fission Q-value for U_{235} and H_{235} = 202.27 MeV is an estimate for the energy deposition per fission (including the additional energy released in capture reactions) in a typical light water reactor.

2.4.2. Mode 1: local energy deposition based on ENDF MT458 data

Similar to mode 0 all energy is deposited at fission sites in mode 1. Energy deposition per fission is calculated based on ENDF MF1 MT458 data [7] which gives components of energy release due to fission as a function of incident neutron energy. More specifically the energy deposition per fission for nuclide i is calculated as

$$E_{\text{fiss},i} = EFR_i + ENP_i + END_i + EGP_i + EGD_i + EB_i + E_{\text{capt}}, \tag{2}$$

where EFR_i is the kinetic energy of the fission products, ENP_i the kinetic energy of the prompt neutrons, END_i the kinetic energy of the delayed neutrons, EGP_i the energy of the prompt gammas, EGD_i the energy of the delayed gammas and EB_i the energy of the delayed betas. E_{capt} is a user-defined constant for additional energy release in capture reactions. The same constant is used for all nuclides and incident neutron energies.

2.4.3. Mode 2: local photon energy deposition

In mode 2 instead of depositing all energy at the fission sites, the neutrons deposit energy along their history in various reactions. The energy of photons is deposited locally at reaction sites. Heating rate due to reactions other than fission is calculated using KERMA (Kinetic Energy Release in MAterials) coefficients, which are obtained by subtracting fission KERMA coefficients from total KERMA coefficients, both of which are produced with NJOY. A clear improvement compared to modes 0 and 1 is the fact that the additional energy release from capture reactions is accounted for explicitly with the KERMA coefficients. Fission energy deposition is calculated separately and the energy deposition per fission for nuclide i is given by

$$E_{\text{fiss},i} = EFR_i + EGP_i + EGD_i + EB_i. \tag{3}$$

2.4.4. Mode 3: coupled neutron-photon transport

This most accurate energy deposition mode uses coupled neutron-photon transport in which secondary photons are produced in neutron collisions based on photon production cross sections and associated energy and angular distributions available in ACE-format cross section libraries. Photon heating is calculated using an analog photon heat deposition tally which is scored after each interaction in which energy is lost: photoelectric effect, Compton scattering and pair production. Similar to mode 2 neutron heating due to reactions other than fission is calculated using KERMA coefficients. In mode 3 the energy deposition per fission for nuclide i is given by

$$E_{\text{fiss},i} = EFR_i + EB_i. \tag{4}$$

As a simple approximation the energy of the delayed fission gammas is deposited with the same distribution as the prompt fission gammas using a method described in [6].

3. TEST CASE

3.1. Serpent Model

The test case is a 3D 15x15 fuel assembly based on TMI fuel assembly design. It contains 204 4.85 % enriched UO_2 pins and 4 Gd_2O_3 + UO_2 burnable poison pins with fuel enrichment of 4.12 % and Gd_2O_3 concentration of 2 %. Boron concentration in the water is 1480 ppm. Reflective boundary condition is used radially and black boundary condition axially. Total power is set to 15.65 MW. The geometry is presented in Figure 1(a).

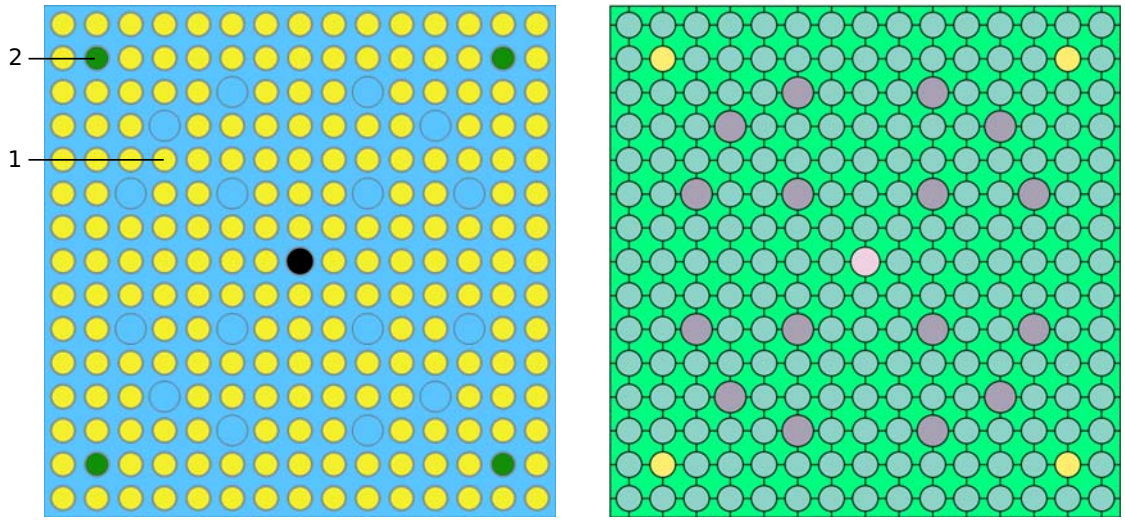

(a) Serpent (b) SCF

Figure 1: Test Case Geometries

3.2. SUBCHANFLOW Model

SCF uses coolant-centered subchannels with 30 axial layers. In total there are 256 channels which are presented in Figure 1(b). The radial temperature distribution in each layer of each fuel pin is solved with 10 radial nodes. Inlet temperature is 565 K, inlet mass flow 85.96 kg/s and outlet pressure 15.5132 MPa.

3.3. Field Tranfer Between Serpent and SCF

The multiphysics interface of Serpent was used for bringing in the density and temperature distribution calculated with SCF and for tallying the energy deposition (power). On-the-fly temperature treatment routine based on Target Motion Sampling (TMS) technique [8] was used for microscopic cross sections. Separate multiphysics interfaces were defined for the coolant and the fuel. A Cartesian mesh based interface was used for the coolant and the 16x16x30 mesh corresponded to the SCF geometry so no interpolation was necessary. Energy deposition to cladding was also tallied using this interface and therefore made a contribution to the coolant power in SCF.

For the fuel a nested mesh based interface was used in order to utilise radial temperature distributions in the fuel pins. On the top level a 15x15x30 Cartesian mesh divided the geometry into cells, each containing one axial layer of one fuel rod. Inside each of these cells a radial division corresponding to the node radii of the SCF fuel temperature solution was defined. During the Serpent calculation the fuel temperature was obtained by linearly interpolating between the temperatures of the two closest nodes based on the radial coordinate. Radial power distributions in the fuel pins were not used in SCF and instead total power in each axial layer of each pin was transferred to SCF.

4. RESULTS

The test case was modelled with energy deposition modes 0, 2 and 3. Mode 1 was not used due to the fact that it offers similar spatial accuracy as mode 0 since in both modes all energy is deposited locally at fission sites. In addition, the user-defined constant E_{capt} is problematic. In order to set an accurate value for this constant the additional energy release in capture reactions per fission would have to be estimated using mode 2 or 3. It should be noted that with all energy deposition modes normalization to total power was used in Serpent which means that only the power distribution varied between the different modes and the total power produced in the problem geometry was the same with all modes.

In each calculation the coupled problem was solved with Picard iteration using 10 coupled iterations. The solution process was started by running a SCF calculation with a cosine shaped axial power distribution in each rod. At each iteration 4×10^8 active neutron histories divided into 2000 cycles of 2×10^5 source neutrons were simulated. On the first iteration 50 inactive cycles were run and on the following cycles the number of inactive cycles was reduced to 20 since the fission source of one transport calculation was used as an initial source for the next transport calculation. A stochastic approximation based relaxation scheme [9] was used for the power and all Serpent calculations were run with ENDF/B-VII.1 based cross section library. With energy deposition mode 3 coupled-neutron photon transport and analog photon production mode were used. This resulted in approximately 9.6×10^9 simulated photon histories during each transport calculation. All of the calculations were run on a computer node consisting of two Ten-Core Intel Xeon E5-2690 v2 3.0 GHz processors with 128 GB RAM memory with a total of 20 OpenMP threads.

The convergence of the coupled calculation was evaluated retrospectively by comparing the fuel temperature distributions on two consecutive iterations. In all four coupled calculations the maximum absolute difference in the fuel temperature distribution was less that 2 K after 10 coupled iterations.

Fuel centreline temperature profiles in two rods (See Figure 1(a) for locations) are presented in Figures 2 and 3. Rod 1 has the highest centreline temperature and rod 2 contains burnable poison. The temperature profiles of these two rods demonstrate well the kind of differences that are observed in the test case in general. Due to symmetry the temperatures of the other three burnable poison rods are similar to the ones of rod 2. The differences in the rods without burnable poison are approximately as high as in rod 1 or lower and the trend in the fuel temperatures between different modes is similar in all of these rods. Coolant temperatures are not presented since the observed differences between the coupled calculations are insignificant.

With mode 2 fuel temperatures are lowered in rod 1 compared to mode 0 and maximum difference compared to mode 0 is 29 K. On the other hand, the use of mode 2 results in higher temperatures for rod 2 with gadolinium and maximum difference compared to mode 0 is 100 K. The increase in the fuel temperatures of rod 2 can be explained by the additional energy release in the capture reactions of gadolinium which is accounted for by the KERMA factors used in mode 2. The decrease in the fuel temperatures of rod 1 can be explained mostly by the fission neutrons which no longer deposit their energy locally at fission sites but instead transport part of this energy out of fuel and deposit it to coolant and cladding. The increased energy deposition in the rods with gadolinium also has a small contribution since the results are normalized to total power.

The use of mode 3 with coupled neutron photon transport results in a decrease in the temperatures of both rods compared to mode 2. For rod 2 the differences in the temperatures compared to mode 0 decrease and the maximum difference is 37 K, which is clearly smaller than the difference of 100 K in mode 2. The main reason for this is the fact that in mode 3 the gammas created in the capture reactions with gadolinium are transported and part of their energy is deposited to materials other than the fuel with gadolinium. Fission gammas from uranium and capture gammas from ^{238}U also deposit a part of their energy to cladding and coolant. This affects also rod 1 and the maximum difference compared to mode 0 is 44 K.

Effective multiplication factors and total calculation times for the three energy deposition modes are presented in Table 1. The one sigma uncertainties for the effective multiplication factors have been taken from the Serpent calculation in the final iteration of each coupled calculation. The effective multiplication factor increases with increasing energy deposition mode. This is probably due to the positive reactivity effect resulting from the decreased fuel temperatures in the rods

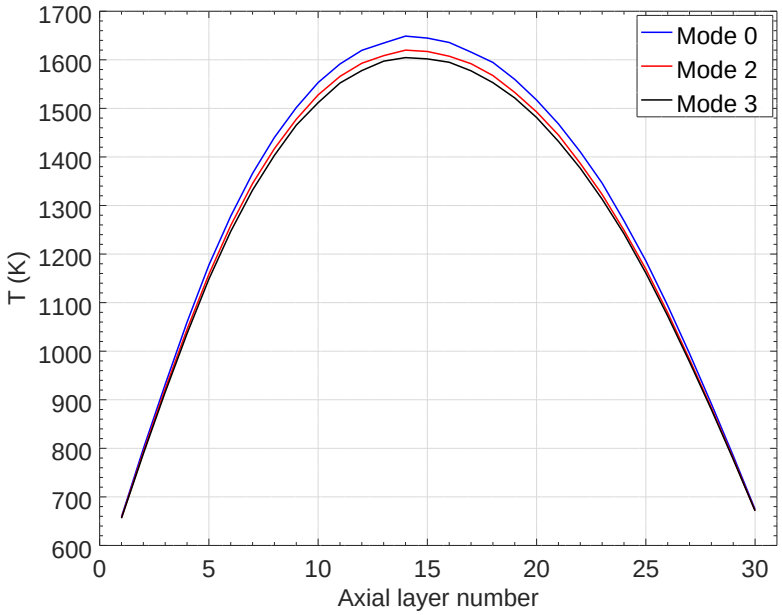

Figure 2: Fuel Centreline Temperature Profile in Rod 1

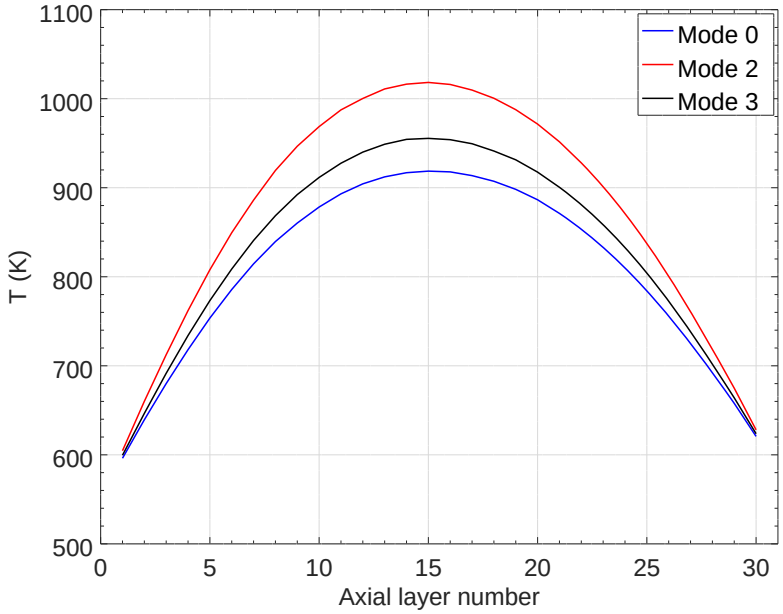

Figure 3: Fuel Centreline Temperature Profile in Rod 2

Table 1: Effective Multiplication Factors and Total Calculation Times

Mode	k_{eff}	Calculation Time (h)
0	1.23773 ± 0.00003	21.7
2	1.23793 ± 0.00003	24.5
3	1.23801 ± 0.00003	37.2

without gadolinium. With mode 2 the calculation time increases by 13 % and with mode 3 by 71 % compared to mode 0.

5. CONCLUSIONS

The effect of energy deposition modelling on coupled steady state Monte Carlo neutronics/thermal hydraulics calculations was studied by modelling a PWR assembly test case with internally coupled Serpent-SUBCHANFLOW code system. A separate coupled calculation was run with three different energy deposition modes of Serpent 2. The calculations resulted in small differences of less than 30 pcm in the effective multiplication factor. The more advanced energy deposition modes 2 and 3 produced slightly lower fuel temperatures for the fuel rods without gadolinium compared to mode 0 in which all energy is deposited in fission. For the gadolinium rods, however, the fuel temperatures are higher when using energy deposition modes 2 or 3.

The test calculation shows that the choice of energy deposition method has a visible effect on

the fuel temperatures. For the highest accuracy energy deposition mode 3 with the coupled neutron photon transport should be used but this results in a significant increase in calculation time compared to the less accurate modes.

The approach presented can be used to estimate the effects of energy deposition approximations on diverse output quantities in various reactor geometries. Serpent can serve as a reference tool both for Monte Carlo codes with approximative energy deposition treatments as well as for deterministic tools.

Finally, it is worth noting that initial limited verification for the new energy deposition treatment was done in [6] but a more thorough verification using code-to-code comparisons is an important part of future work. This is however a challenging task since the number of publications with accurate energy deposition calculations is small. Needless to say, the methods should also be validated against measurement data.

ACKNOWLEDGEMENTS

This work has been funded from the McSAFE project which is receiving funding from the Euratom research and training programme 2014-2018 under grant agreement No 755097.

REFERENCES

[1] J. Leppänen, M. Pusa, T. Viitanen, V. Valtavirta, and T. Kaltiaisenaho. "The Serpent Monte Carlo code: Status, development and applications in 2013." *Annals of Nuclear Energy*, **volume 82**, pp. 142–150 (2015).

[2] T. Kaltiaisenaho. "Implementing a photon physics model in Serpent 2." M.Sc. Thesis, Aalto University, 2016. (2016).

[3] J. Leppänen, V. Hovi, T. Ikonen, J. Kurki, M. Pusa, V. Valtavirta, and T. Viitanen. "The Numerical Multi-Physics project (NUMPS) at VTT Technical Research Centre of Finland." *Annals of Nuclear Energy*, **volume 84**, pp. 55–62 (2015).

[4] U. Imke and V. H. Sanchez. "Validation of the subchannel code SUBCHANFLOW using the NUPEC PWR tests (PSBT)." *Science and Technology of Nuclear Installations*, **volume 2012** (2012).

[5] D. Ferraro, M. García, V. Valtavirta, U. Imke, R. Tuominen, J. Leppänen, and V. Sanchez-Espinoza. "Serpent/SUBCHANFLOW pin-by-pin coupled transient calculations for a PWR minicore." *Annals of Nuclear Energy*, **volume 137**, p. 107090 (2020).

[6] R. Tuominen, V. Valtavirta, and J. Leppänen. "New energy deposition treatment in the Serpent 2 Monte Carlo transport code." *Annals of Nuclear Energy*, **volume 129**, pp. 224 – 232 (2019).

[7] A. Trkov, M. Herman, and D. A. Brown. "ENDF-6 Formats Manual – Data Formats and Procedures for the Evaluated Nuclear Data Files ENDF/B-VI, ENDF/B-VII and ENDF/B-VIII." Technical Report BNL-203218-2018-INRE, Brookhaven National Laboratory (2018).

[8] T. Viitanen. "Development of a stochastic temperature treatment technique for Monte Carlo neutron tracking." D.Sc. Thesis, Aalto University, 2015. (VTT Science 84) (2015).

[9] J. Dufek and W. Gudowski. "Stochastic approximation for Monte Carlo calculation of steady-state conditions in thermal reactors." *Nuclear science and engineering*, **volume 152**(3), pp. 274–283 (2006).